Progress towards ignition on the National Ignition Facility

Progress towards ignition on the National Ignition Facility

J.D. Lindl[1], L.J. Atherton[1], P.A. Amendt[1], S. Batha[3], P. Bell[1], R.L. Berger[1], R. Betti[2], D.L. Bleuel[1], T.R. Boehly[2], D.K. Bradley[1], D.G. Braun[1], D.A. Callahan[1], P.M. Celliers[1], C.J. Cerjan[1], D.S. Clark[1], G.W. Collins[1], R.C. Cook[1], E.L. Dewald[1], L. Divol[1], S.N. Dixit[1], E. Dzenitis[1], M.J. Edwards[1], J.E. Fair[1], R.J. Fortner[1], J.A. Frenje[5], V.Yu. Glebov[2], S.H. Glenzer[1], G. Grim[3], S.W. Haan[1], A.V. Hamza[1], B.A. Hammel[1], D.R. Harding[2], S.P. Hatchett[1], C.A. Haynam[1], H.W. Herrmann[3], M.C. Herrmann[4], D.G. Hicks[1], D.E. Hinkel[1], D.D. Ho[1], N. Hoffman[3], H. Huang[6], N. Izumi[1], B. Jacoby[1], O.S. Jones[1], D.H. Kalantar[1], R. Kauffman[1], J.D. Kilkenny[6], R.K. Kirkwood[1], J.L. Kline[3], J.P. Knauer[2], J.A. Koch[1], B.J. Kozioziemski[1], G.A. Kyrala[3], K. La Fortune[1], O.L. Landen[1], D. Larson[1], R. Lerche[1], S. Le Pape[1], R. London[1], B.J. MacGowan[1], A.J. MacKinnon[1], T.N. Malsbury[1], E.R. Mapoles[1], M.M. Marinak[1], P.W. McKenty[2], N. Meezan[1], D.D. Meyerhofer[2], P. Michel[1], J. Milovich[1], J.D. Moody[1], M. Moran[1], K.A. Moreno[6], E.I. Moses[1], D.H. Munro[1], A. Nikroo[6], R.E. Olson[4], T. Parham[1], R.W. Patterson[1], K. Peterson[4], R. Petrasso[5], S.M. Pollaine[1], J.E. Ralph[1], S.P. Regan[2], H.F. Robey[1], M.D. Rosen[1], R. Sacks[1], J.D. Salmonson[1], T.C. Sangster[2], S.M. Sepke[1], D.H. Schneider[1], M.B. Schneider[1], M. Shaw[1], B.K. Spears[1], P.T. Springer[1], C. Stoeckl[2], L.J. Suter[1], C.A. Thomas[1], R. Tommasini[1], R.P. Town[1], B.M. VanWonterghem[1], R. Vesey[4], S.V. Weber[1], P.J. Wegner[1], K. Widman[1], C.C. Widmayer[1], M. Wilke[3], H.L. Wilkens[6], E.A. Williams[1], D.C. Wilson[3] and B.K. Young[1]

[1] Lawrence Livermore National Laboratory, Livermore, CA, 94551, USA
[2] Laboratory for Laser Energetics, Rochester, NY, USA
[3] Los Alamos National Laboratory, Los Alamos, NM, USA
[4] Sandia National Laboratory, Albuquerque, NM, USA
[5] Plasma Science and Fusion Center, MIT, Cambridge, MA, 02139, USA
[6] General Atomics, San Diego, CA, USA

E-mail: lindl1@llnl.gov

Abstract
The National Ignition Facility at Lawrence Livermore National Laboratory was formally dedicated in May 2009. The hohlraum energetics campaign with all 192 beams began shortly thereafter and ran until early December 2009. These experiments explored hohlraum-operating regimes in preparation for experiments with layered cryogenic targets. The hohlraum energetic series culminated with an experiment that irradiated an ignition scale hohlraum with 1 MJ. The results demonstrated the ability to produce a 285 eV radiation environment in an ignition scale hohlraum while meeting ignition requirements for symmetry, backscatter and hot electron production. Complementary scaling experiments indicate that with $\sim$1.3 MJ, the capsule drive temperature will reach 300 eV, the point design temperature for the first ignition campaign. Preparation for cryo-layered implosions included installation of a variety of nuclear diagnostics, cryogenic layering target positioner, advanced optics and facility modifications needed for tritium operations and for routine operation at laser energy greater than 1.3 MJ. The first cyro-layered experiment was carried out on 29 September 2010. The main purpose of this shot was to demonstrate the ability to integrate all of the laser, target and diagnostic capability needed for a successful cryo-layered experiment. This paper discusses the ignition point design as well as findings and conclusions from the hohlraum energetics campaign carried out in 2009. It also provides a brief summary of the initial cryo-layered implosion.

(Some figures in this article are in colour only in the electronic version)

1. Ignition point design

The National Ignition Facility (NIF) [1, 2] at Lawrence Livermore National Laboratory is a 192 beam, 1.8 MJ 0.35 μm laser designed to drive inertial confinement fusion (ICF) capsules to ignition [3–5]. NIF was formally dedicated in May 2009. The National Ignition Campaign, a collaborative research undertaking by LLNL, LLE, LANL, GA and SNL, has a goal of achieving a robust burning plasma by the end of 2012. In the indirect-drive approach [6, 7], the laser energy is converted to thermal x-rays inside a high Z cavity (hohlraum). The x-rays then ablate the outer layers of a DT-filled capsule placed at the centre of the hohlraum, causing the capsule to implode, compress and heat the DT and ignite.

Computer models of the implosion using the codes LASNEX [8] and HYDRA [9], developed over the course of the US ICF Program, are extensively utilized to specify the point design target and the experiments required for the optimization of the implosion. Figure 1(*a*) shows a schematic of the point design hohlraum, figure 1(*b*) shows the capsule design for the first ignition campaign and figure 1(*c*) shows the laser pulse.

An extensive discussion of the point design and the methodology developed to establish specifications on the target, the laser and the experimental campaign can be found in [10]. Fabrication of the target is discussed in [11] and laser performance is discussed in [12]. The hohlraum is a 1 cm-long, 5.44 mm diameter cylindrical hohlraum, designed with Au walls for current experiments and filled with 0.9 mg cm^{-3} of He tamping gas. The hohlraum has two laser entrance holes (LEH) of ≈55–60% of the hohlraum diameter. Details of the LEH and other features of the target will be finalized to optimize performance based on the results of ongoing experiments. To achieve x-ray irradiation symmetry, 24 sets of beams arranged in quads of 4 beams each enter an LEH from each end of the hohlraum in sets of 4, 4, 8 and 8 at 23.5°, 30°, 44.5° and 50° from the hohlraum symmetry axis. The hohlraum is driven by a 1.3 MJ, 20 ns-long shaped pulse designed to implode the cryogenic fuel layer to a density in excess of 1000 g cm^{-2}. The current design [10] for the cryogenic capsule at hohlraum centre is a graded Ge-doped [13, 14] CH ablator of 918 μm inside radius and 190 μm shell thickness enclosing a 68 μm thick layer of solid DT fuel initially held near the triple point [15].

Laser requirements for ignition experiments on the NIF are set by two principal physics constraints. First, laser–plasma interaction (LPI) effects limit the power and energy that can be delivered to a target while maintaining precise control of the temporal and spatial distribution of the deposition of that energy. This limit on the power and energy puts a limit on the pressure that can be generated during the implosion of a shell containing the fusion fuel. Second, at a given maximum pressure, hydro-instabilities set a maximum velocity to which the fuel can be accelerated and this maximum velocity establishes the minimum fuel mass and driver energy required for ignition. Based on over two decades of experiments on the Nova and Omega lasers, NIF was designed and built to achieve ignition under these constraints.

The fundamental input variables of an ICF implosion are the implosion velocity (V), fuel entropy (S) or adiabat (α), the

shape of the central hot spot (S_{hs}) and the mix (M) of capsule and ablator on the outer surface of the dense fuel. Based on a comparison of the computer models with past experimental results, we have identified 14 laser and 3 target parameters shown in figure 2 which must be set precisely in experiments in order to optimize these key quantities in the imploded fuel assembly as required for ignition.

Based on these input variables, we have developed an input ignition threshold factor (ITF) which describes the requirements for ignition. ITF is equivalent to a generalized Lawson criterion for ICF [16, 17] and is given by the formula [10]

$$
\text{ITF} = I_0 \left(\frac{M_{\text{DT}}}{M_0} \right) \left(\frac{v}{v_0} \right)^8 \left(\frac{\alpha}{\alpha_0} \right)^{-4} \left(1 - 1.2 \frac{\Delta R_{\text{hotspot}}^{\text{K-wtd}}}{R_{\text{hotspot}}} \right)^4
$$

$$
\times \left(\frac{M_{\text{clean}}}{M_{\text{DT}}} \right)^{0.5} (1 - P_{\text{hs}}).
$$

ITF is a dimensionless quantity that is normalized to be unity when the expected thermonuclear yield equals the input laser energy. ITF is a measure of margin, and we define the margin as ITF-1. I_0 is the ITF of the baseline optimized 1D implosion. It is about 4 for the point design shown in figure 1. The velocity v provides the kinetic energy for compression and heating. The adiabat α—the ratio of the pressure required to reach a given density compared with that required for a Fermi degenerate compression—determines how efficiently that kinetic energy can be used to generate the required total ρR and hotspot conditions. Quantities with subscript zero are nominal values for the point design. For the ignition design shown in figure 1, $v_0 = 370$ km s^{-1} and $\alpha_0 = 1.5$. If the implosion had nominal values of v and α, and were 1D—that is, $\Delta R_{\text{hotspot}}^{\text{K-wtd}}$ is zero and $M_{\text{clean}} = M_{\text{DT}}$—then it would have I_0 times more fuel mass M_{DT} than required for ignition. One can use up that factor of about 4 by reducing any of the terms until ITF is unity, at which point the expected gain is unity. In this equation, $\Delta R_{\text{hotspot}}^{\text{K-wtd}}$ is the RMS deviation of the central hot spot from spherical. Non-spherical hot spots produce less yield and reduce the margin of a 1D implosion.

Similarly, $M_{\text{clean}}/M_{\text{DT}}$ is the fraction of the fuel which contains less than 5% by mass of any ablator material which might have mixed into the main fuel layer during the implosion. Mix of ablator into the fuel reduces compressibility and dilutes the fuel. P_{hs} is a measure of the purity of the hot spot and accounts for mix which penetrates all the way through the main fuel layer into the central gas region. This deep mix can cool the hot spot and reduce its yield. ITF is discussed in great detail in [10]. Because of variability from shot to shot in the target and laser, and because of uncertainty in setting the key implosion parameters, there will be a range of ITF that will be achieved on any given shot. We have explored the expected distribution of ITF and the resulting target performance in an ensemble of 2D calculations which vary the laser, target and experimental inputs within the ranges set by the point design specifications. The result of this ensemble of calculations is shown in figure 3(*a*) for expected variations of the Rev5-CH point design shown in figure 1 and described more fully in [10]. In this figure, black dots are for calculations which meet the specifications for variability in the laser, target and experimental inputs. The red dots are
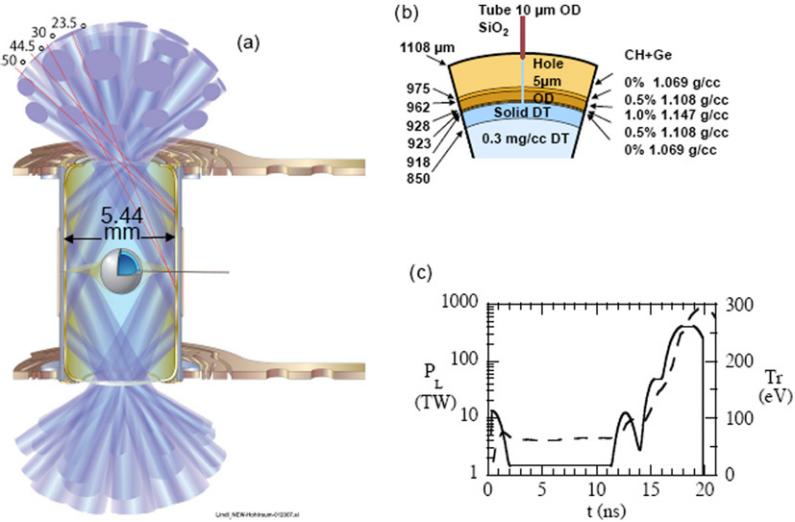
Figure 1. (*a*) Schematic of the 300 eV CH indirect-drive ignition target. (*b*) Capsule cross-section. (*c*) Total laser power (solid) and radiation temperature T_r at capsule (dashed) versus time.
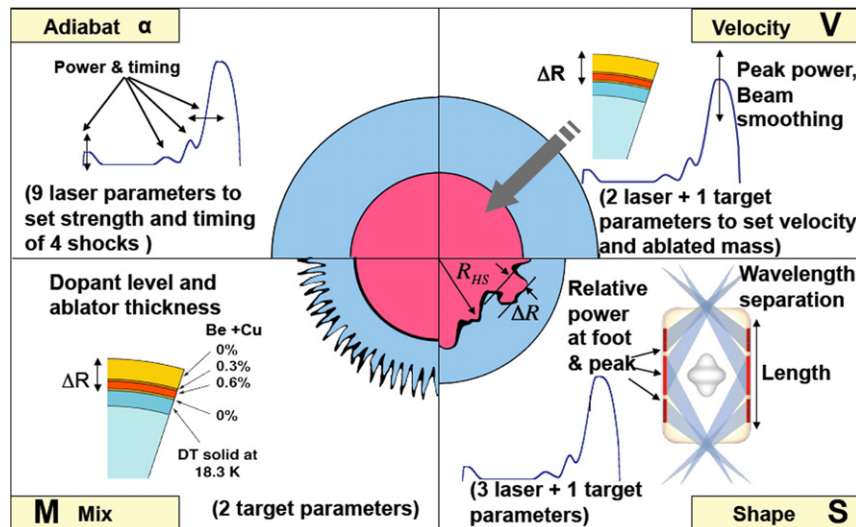

Figure 2. To compensate for physics uncertainties, the experimental campaign will set 14 laser and 3 target parameters to optimize V, adiabat α, ablator/fuel, mix and hot spot shape.

for calculation which fall outside the specifications but which represent the wider variation expected early in the ignition campaign. As discussed above, at its nominal 1D performance, the point design in figure 1 would have an ITF of about 4. We have set the specifications such that, in the presence of this variability and measurement uncertainty in the experiments, we expect the point design to have an ITF > 1 following a successful implosion optimization campaign. For this ignition design, we expect about 2/3 of the shots to have a yield above 1 MJ and a median yield of about 8 MJ, if we meet all of the specifications during the ignition campaign. These estimates will evolve as we obtain data in the experimental campaign and we can compare measured performance and variability with our current expectations. Shown in figure 3(*b*) is an equivalent formulation of the ignition factor, ITFX, based on the observable outputs of the implosion. This will be discussed below.

The point design target shown in figure 1 is designed to operate at a radiation temperature of 300 eV. Alternate ignition

designs exist which span a range from 270 to 300 eV [18–23]. One of the most complex and challenging issues for ignition is the radiation temperature that can be achieved while meeting the ignition design requirements for drive, symmetry and capsule preheat from hot electrons generated by LPI processes, the most important of which in hohlraums is stimulated Raman scattering (SRS).

2. Hohlraum energetics campaign

The hohlraum energetics campaign [24] with all 192 beams, began shortly after NIF dedication and ran until early December 2009. These experiments explored hohlraum-operating regimes in preparation for experiments with layered cryogenic targets, the first of which was carried out on 29 September 2010. The rest of this paper summarizes the hohlraum energetics series and the first cyro-layered experiment including the capabilities which had to be developed to carry out these experiments.
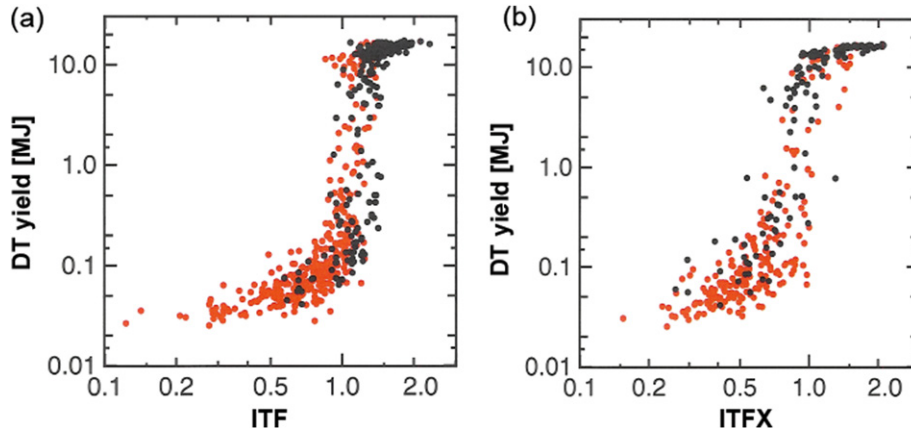
Figure 3. In this figure, black dots are for 2D calculations which meet the specifications for variability in the laser, target and experimental inputs. The red dots are for calculation which fall outside the specifications but which represent the wider variation expected early in the ignition campaign. (*a*) Yield versus the ignition threshold factor (ITF) based on the inputs to an implosion, (*b*) yield versus an equivalent metric ITFX, based on observables of low yield THD implosions.
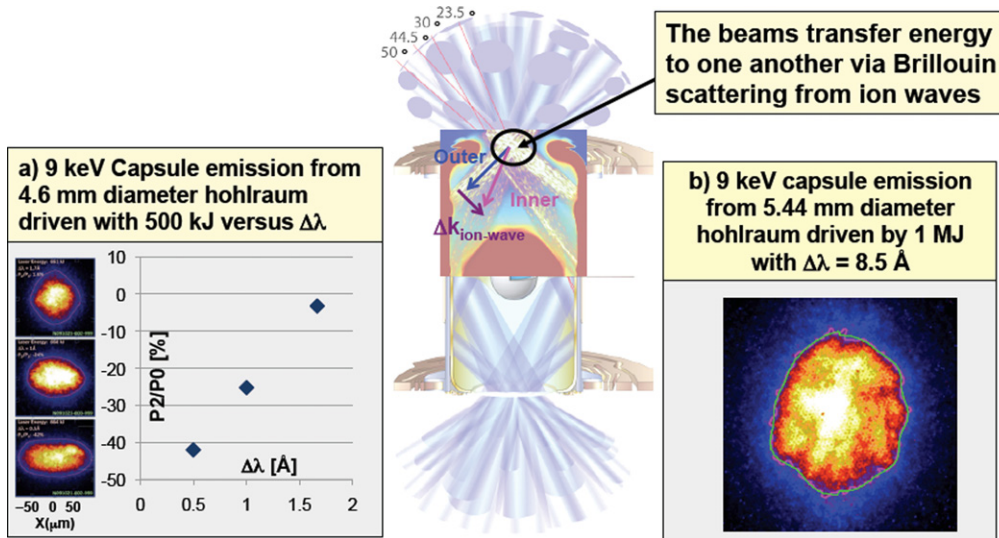

Figure 4. We demonstrated the ability to control implosion symmetry, using a 'plasma-optical-switch' to transfer energy from outer to inner beams by increasing $\Delta\lambda = \lambda_{\text{inners}} - \lambda_{\text{outers}}$.

Initial experiments in the hohlraum energetics campaign began at 500 kJ into a reduced scale hohlraum whose diameter and length were 0.86 those of the ignition hohlraum. The reduced energy was chosen so that we could gain operational experience with NIF before moving to higher energies. The series culminated with an experiment that irradiated an ignition scale hohlraum with 1 MJ, approximately thirty times the energy that any laser driven hohlraum has been irradiated previously. The results demonstrated the ability to produce a 285 eV radiation environment in an ignition scale hohlraum while meeting ignition requirements for symmetry, backscatter and hot electron production. Complementary scaling experiments indicate that with 1.3 MJ, the capsule drive temperature will reach 300 eV, the point design temperature for the ignition target in figure 1.

Radiation symmetry in NIF hohlraums is controlled by adjusting the relative powers between the inner beams at 23.5° and 30° and the outer beams at 44.5° and 50° or by changing the hohlraum length relative to its diameter. Controlling radiation symmetry has been a key aspect of ICF research on both the

Nova and Omega lasers [6, 7]. The relative power between inner and outer beams can be varied directly by varying input power in the beams. This approach was demonstrated in a wide variety of experiments on Omega and is one of the techniques being used on NIF. However, on NIF, we also demonstrated the ability to control symmetry by transferring energy from outer to inner beams by changing their relative frequency by a few angstroms [24, 25].

This novel cross-beam transfer is due to three-wave mixing [26, 27] where the beams cross in the flowing LEH plasmas. To utilize this approach to symmetry control, we employed different oscillators for the inner beams and the outer beams. Figure 4(*a*) shows the results of using this technique on the 4.6 mm diameter reduced scale hohlraum at an input energy of ∼500 kJ. Shown are 9 keV x-ray images taken using the Gated X-ray Diagnostic (GXD) [28] at peak x-ray brightness near the minimum radius of the implosion. This GXD takes a sequence of 70 ps images, separated in time by about 30 ps using an array of pinholes. This symmetry tuning technique was also demonstrated at 660 kJ in the 4.6 mm reduced scale
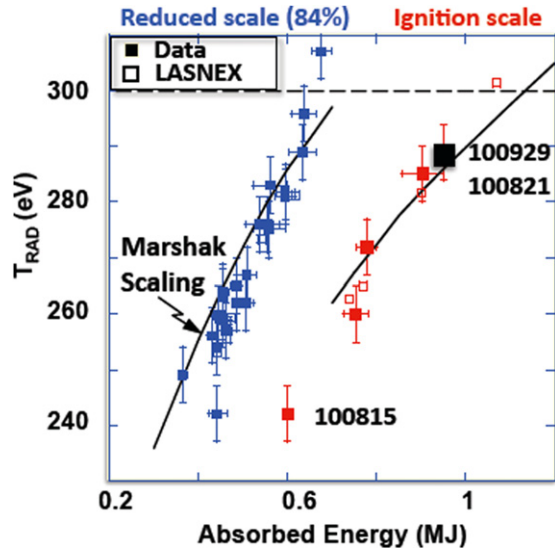
Figure 5. Radiation temperatures versus laser energy in NIF scale hohlraums follow a simple Marshak scaling law. The temperatures are also consistent with LASNEX calculations. Red points are for a 5.44 mm diameter ignition scale hohlraum. Blue points are for a 4.6 mm diameter hohlraum.

hohlraum and then applied successfully at 1 MJ into a full scale ignition hohlraum. The larger scale ignition hohlraums required about a 8.5 Å frequency shift to obtain the proper energy distribution in the hohlraum. Symmetry in ignition scale hohlraums, shown in figure 4(*b*) for the December 2009 megajoule shot, will be further optimized in the implosion optimization campaign in 2011.

Besides demonstrating the ability to control symmetry at the megajoule scale, the hohlraum energetics campaign demonstrated ∼90% laser–plasma absorption using back-scatter [29] and near backscatter [30] optical diagnostics on a 30° and 50° beam quad, hot electron levels using a filter-fluorescer diagnostic [31] which meet the ignition target specifications [10] and peak hohlraum thermal x-ray production at expected levels using the multi-channel soft x-ray power diagnostic Dante [32]. Figure 5 shows radiation temperature versus laser energy for the ignition scale 5.44 mm diameter hohlraum and the subscale 4.6 mm diameter hohlraum. These temperatures follow the expectations from a simple Marshak scaling [6] as discussed by Glenzer *et al* [33] and are also consistent with Lasnex calculations as shown. Based on analysis of these results, we expect to be able to further optimize hohlraum performance. Calculations indicate that we would be able to achieve symmetry with less cross beam transfer with a slightly shorter hohlraum, and that the cross-beam transfer can be further optimized using a third oscillator [34]. In addition, we intend to image hard x-ray emission from the capsule to better quantify the fraction of preheat electron which reach the capsule.

3. THD cryo-layered implosion

The second stage of the ignition campaign involves utilizing this hohlraum to achieve the fuel conditions required for ignition. The key implosion parameters discussed above will be optimized in a set of specialized targets without cryogenic

fuel layers as discussed extensively in [35]. The results of these experiments will be integrated into cyro-layered targets. These cryo-layered targets will initially be designed for low yield using a fuel layer composition consisting mainly of tritium and hydrogen with only a few per cent deuterium, referred to as THD layers. These targets and their expected performance are discussed extensively in [36]. Using these low yield targets, we will be able to maintain the full array of diagnostics needed to optimize the fuel assembly before shifting to a 50/50 DT layer to achieve ignition.

We find that the performance of these THD targets can be a good predictor of DT performance. As shown in figure 3(*b*), the parameter:

$$\text{ITFX} = I_{x0} \left(\frac{m}{m_{\text{DT}}} \right) \left(\frac{Y}{Y_0} \right) \left(\frac{\text{DSR}}{\text{DSR}_0} \right)^{2.3}$$

is found to be a good predictor of DT performance. Y is the measured neutron primary yield (defined as the integral between 13–15 MeV) and m_{DT} is the fuel mass. The DSR is the measured neutron down-scattered ratio (defined as the number of neutrons between 10 and 12 MeV expressed as a fraction of those between 13 and 15 MeV). These are the primary DT neutrons down scattered to lower energy by scattering in the fuel surrounding the central hot spot. The DSR is proportional to the total fuel ρR. The precise limits on the energy range of the DSR are not found to be critical as long as the neutrons can be clearly distinguished from the TT neutrons. The constant I_{X0} is the mean value of ITFX. At ITFX = 1, as for ITF = 1, the probability of achieving gain ⩾1 is 50%, where gain is defined as the ratio of the energy produced by the burning capsule to the laser energy into the hohlraum. The constants Y_0 and DSR_0 are the mean values for yield and DSR. The value of these quantities and their expected variability is discussed extensively in the paper by Edwards *et al* [36].

Preparation for the THD implosions has required installation of a variety of nuclear diagnostics, cryogenic layering target positioner, advanced optics and facility modifications needed for tritium layered targets and for routine operation at laser energy greater than 1.3 MJ. Installation of this equipment was a major focus of NIF during the first nine months of 2010. Figure 6 shows the cryo-tarpos, the target positioner that was developed to allow the formation of cryogenic layers just outside the NIF target chamber prior to insertion of the target into the chamber.

Figure 7 shows the tip of the cry-tarpos positioner arm including the partially open cryogenic shroud, which retracts a few seconds before shot time after the target is inserted into the chamber centre. Also shown is the cryogenic target for the first cryogenic layered experiments attached to the positioner. Figure 8(*b*) shows a NIF hohlraum designed for layering experiments. It includes a pair of viewing windows at the waist of the hohlraum. These viewing windows, and the LEH provide access for x-ray phase contrast imaging of the layer, from three directions, as the layer forms. The fuel layer and the capsule ablator can be seen in such an image as shown in figure 8. The Hohlraum is fitted with two silicon arms at each end of the hohlraum to set the hohlraum-operating temperature, and a pair of trim heating coils just inside of each arm for fine tuning of the low mode symmetry of the layer.

Figure 6. Cryo-tarpos enables the formation of cryogenic layers just outside the NIF target chamber.
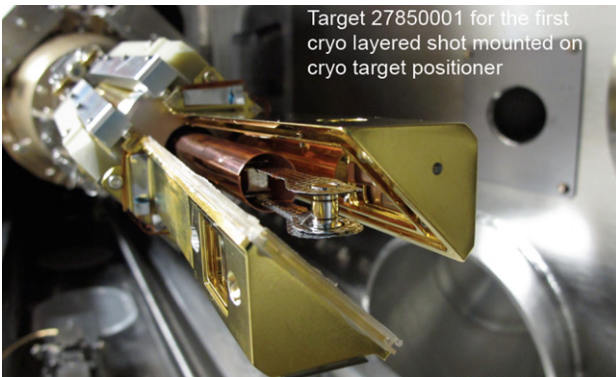

Figure 7. Cryogenic shroud and target for the first THD shot on NIF.

By taking a sequence of x-ray images, we can watch the layer develop in time.

A wide range of new diagnostics was fielded on the first THD shot. This included several neutron time of flight detectors (NTOF) [37–41] at different distances from the chamber which will be used to measure the primary DT neutron yield and azimuthal variations, burn averaged ion temperature and the fraction of neutrons scattered by the fuel, the DSF discussed above, which is proportional to ρR.

A number of detectors are required to cover the large range in neutron yields for THD and DT implosions. Several detectors located at ∼4 m from the target chamber center (TCC) are utilized for yield, ion temperature and time of peak neutron emission (bang time) for the lower yield THD targets. An additional two detectors will be located at ∼20 m from TCC. These allow the neutron signal to dilate in time making it easier to measure the spectrum for the DSR. For DT yields with 50/50 fuel mixtures, the close in detectors will no longer work and the 20 m detectors are relied on for all spectral information. The neutron spectrum will also be measured using a magnetic recoil spectrometer [42] (MRS), which provides an additional line of sight. This converts the neutron signal to a proton signal via collisions in a CH target foil. The proton spectrum is then measured by dispersing them spatially on to CR39 using a magnet. This diagnostic has been designed to work for the entire range of neutron yields from THD and DT targets.

Neutron activation detectors containing zirconium [Zr90(n,2n)Zr89] will measure yield at several different azimuths to complement the NTOF, and MRS detectors. The threshold energy for activation is ∼12 MeV making this suitable for measuring the primary DT neutron signal. The yield is inferred by measuring absolutely the ∼909 keV γ-ray yield from the activated Zr nuclei. This is similar to the copper activation technique also employed on NIF, but unlike Cu the Zr has a much longer half-life (∼3 days versus 10 min) making it functionally easier to implement.

Other new instruments included a Gamma Reaction History (GRH) or 'burn history' diagnostic which is a 4-channel gas Cherenkov γ-ray detector [43] located 6 m from TCC. The γs impact a converter foil producing electrons, which then produce Cerenkov radiation in the gas cells. The four cells will have different gas densities to produce gamma thresholds of 3, 5, 8 and 14 MeV. Data from these channels will be used to obtain the total yields and time history of three capsule gamma rays; 16.7 MeV gamma rays from a branch of the D+T reaction, 19.8 MeV from T+H reaction and 4.4 MeV from neutrons interacting with the carbon in a plastic ablator.

A key feature of the THD implosions is that the neutron yield can be controlled via the %D concentration in the fuel to optimize the diagnostics environment. It is expected that x-ray imaging will be feasible on NIF, without special relay optics to a shielded location, for neutron yields up to ∼10^{15} using a hardened gated x-ray imager [44]. Similar to the GXD used in the hohlraum energetics campaign, this imager provides a large number of snapshots of the implosion for hot spot size and shape. Each image integrates over ∼35–70 ps, and a total interval ∼800 ps can be covered, compared with the 100 ps of the THD emission time. The spatial resolution is ∼5–10 μm compared with the ∼25 μm diameter of the x-ray image at peak brightness. Different filtering can be used to provide spectral discrimination on the same shot in order to extract temperature information [45, 46]. A similar diagnostic, being built to operate in the 10^{17} range for implosions with higher %D fills, must be located outside the target chamber with adequate shielding against the higher neutron environment. A faster camera is under development to provide ∼10 ps resolution, which is of the same order as the burn width of igniting targets. NIF will soon have a neutron imager which will also provide time integrated spatial information of the hot spot [47]. The detector will be a stacked fibre scintillator located 28 m from the target, imaged by two cameras to produce one image of the primary neutrons, between ∼13 and 20 MeV, and another gated from 10 to 12 MeV showing neutrons scattered within the capsule.

Bringing together all of these new diagnostics, as well as the cryo-target positioner and all of the additional infrastructure needed to carry out experiments with tritium in such a short period of time was a major undertaking. The main purpose of the first THD cryo-layered experiment was to demonstrate the ability to integrate all laser, target and diagnostics capabilities needed for a successful experiment. The experiment carried out on 29 September fully demonstrated this capability. As shown by the black square in figure 5, the hohlraum achieved a radiation temperature of nearly 290 eV, consistent with expectations from the earlier non-layered hohlraum energetics series. However, we have done none of the optimization of
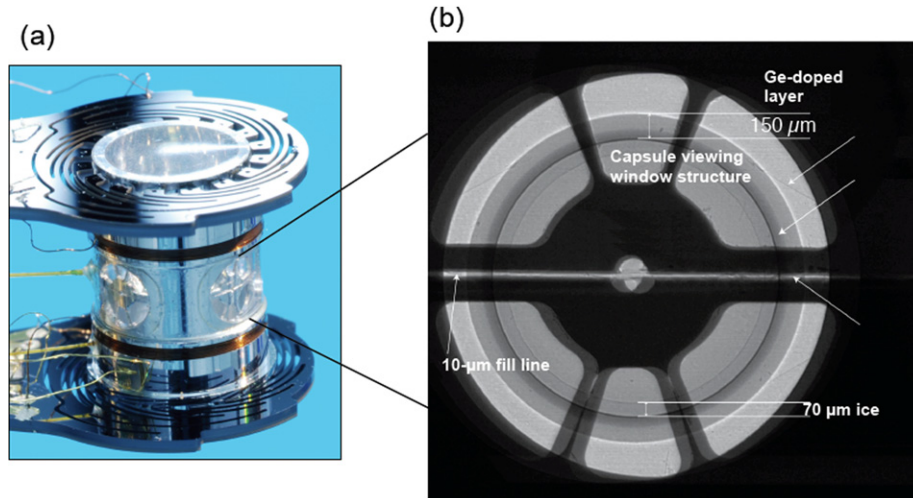
Figure 8. (*a*) Cryo-layering hohlraum, (*b*) cryo fuel layers are imaged with x-rays from three directions through slots in the hohlraum at the hohlraum waist and through the LEH.
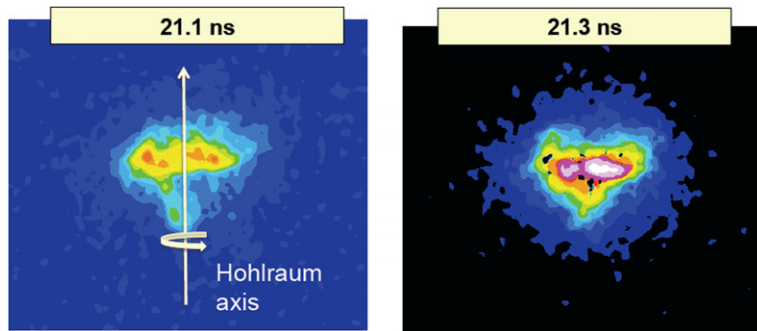

Figure 9. A pair of GXD images from the THD shot near peak emission shows a jet of material passing through and cooling the hot spot.

symmetry, shock timing, velocity or mix that will be required for THD capsules to reach the yield and DSR required for a DT capsule to ignite.

Figure 9 shows a pair of 9 keV GXD x-ray images taken near peak emission for the THD shot. The implosion was 'pancaked' along the hohlraum axis. These data indicate that in future THD shots we will need to improve the low mode symmetry as was done for the non-layered implosions discussed above. Convergence ratios in THD implosions are a factor of two or more larger than for the non-layered implosions so the radiation flux and low mode capsule and cryo-layer uniformity must be proportionately better. Also there is a jet of material seen in the two images in figure 9. In the full sequence of images from the GXD, this jet passes through the hot spot. The jet is likely to have been generated by hydrodynamic instability growth of an isolated defect on the surface of the capsule. These data indicate that there is work to be done to further improve capsule surface features arising from dust and other assembly artefacts. Optimization of the THD fuel assembly using the surrogate tuning targets discussed above along with the THD implosions will be the focus of the coming year for the NIC.

The goal of the NIC campaign is a robust ignition target by the end of 2012. When successful, the ignition targets being explored by NIC will lay the ground work for targets which meet the performance requirements for energy production for inertial fusion (IFE).
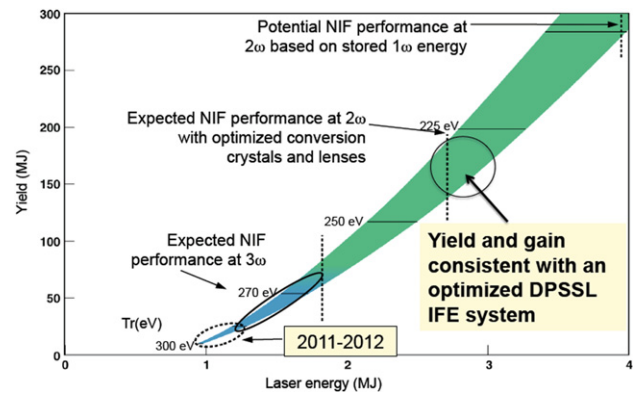

Figure 10. Ignition experiments in 2011–2012 are expected to lay the groundwork for target performance which meets the IFE requirement.

The expected performance of such targets is shown in figure 10. This gain curve is based on direct extensions of NIC targets, keeping ITF constant as they move to higher laser energy and yield. At larger size, these targets have relatively more fuel and yield than the smaller NIC targets because they can ignite at lower velocity [6]. In addition to the initial CH point design, the NIC will explore higher performing targets at higher laser energy or with more efficient ablators, including Be and high density carbon (HDC) [48]. NIF will be able to explore these targets up to energies of 1.8 MJ of 3ω

light at 0.35 μm. Because larger yield targets require lower implosion velocity, they can be imploded at lower hohlraum temperature and require correspondingly lower laser intensity in the hohlraum. NIF is capable of producing ∼3 MJ or more of 2ω light at 0.53 μm as indicated in figure 10. Depending on the outcome of LPI experiments to be conducted at 2ω on NIF, it may be possible to achieve adequate hohlraum temperatures for these larger targets using this longer wavelength. If so, NIF would be able to explore the full range of targets needed for IFE.

4. Summary

Initial hohlraum energetics experiments put us into the hohlraum temperature range for ignition experiments at 280–300 eV. The laser, diagnostic, target fabrication, cryo-layering target positioner and other infrastructure capabilities needed for the ignition campaign are now in place. We have carried out the first THD cryo-layered implosion demonstrating the ability to integrate all of these capabilities. Based on our current understanding, following a successful tuning campaign, we will have a high probability of ignition with yields expected to be in the range 5–10 MJ using CH capsules and hohlraums which require about 1.3 MJ of laser energy. We expect these early ignition experiments to lay the ground work for target performance which meets the IFE requirement.

Acknowledgment

References

[1] Miller G.H., Moses E.I. and Wuest C.R. 2004 *Nucl. Fusion* **44** 228
[2] Moses E.I., Boyd R.N., Remington B.A., Keane C.J. and Al-Ayat R. 2009 *Phys. Plasmas* **16** 041006
[3] Moses E.I. 2008 *J. Phys.: Conf. Ser.* **112** 012003
[4] Kilkenny J.D., Bernat T.P., Hammel B.A., Kauffman R.L., Landen O.L., Lindl J.D., Macgowan B.J., Paisner J.A. and Powell H.T. 1999 *Laser Part. Beams* **17** 159
[5] Kilkenny J.D. *et al* 1999 *Phil. Trans. R. Soc. Lond.* A **357** 533
[6] Lindl J.D. 1995 *Phys. Plasmas* **2** 3933
[7] Lindl J.D., Amendt P., Berger R.L., Glendinning S.G., Glenzer S.H., Haan S.W., Kauffman R.L., Landen O.L. and Suter L.J. 2004 *Phys. Plasmas* **11** 339
[8] Zimmerman G.B. and Kruer W.L. 1975 *Comment. Plasma Phys. Control. Fusion* **2** 51
[9] Marinak M.M. *et al* 1996 *Phys. Plasmas* **3** 2070
[10] Haan S.W. *et al* 2011 Point design targets, specifications, and requirements for the 2010 ignition campaign on the National Ignition Facility *Phys. Plasmas* at press
[11] Atherton L.J. 2008 *J. Phys.: Conf. Ser.* **112** 032063
[12] Haynam C.A. *et al* 2007 *Appl. Opt.* **46** 3276
[13] Clark D.S., Haan S.W., Hammel B.A., Salmonson J.D., Callahan D.A. and Town R.P.J. 2010 *Phys. Plasmas* **17** 052703
[14] Suter L.J. *et al* 2005 *Phys. Plasmas* **12** 056316
[15] Sangster T.C. *et al* 2007 *Phys. Plasmas* **14** 058101
[16] Zhou C.D. and Betti R. 2008 *Phys. Plasmas* **15** 102707
[17] Chang P., Betti R., Spears B.K., Anderson K.S., Edwards J., Fatenejad M., Lindl J.D., McCrory R.L., Nora R. and Shvarts D. 2010 *Phys. Rev. Lett.* **104** 135002
[18] Wilson D.C. *et al* 1998 *Phys. Plasmas* **5** 1953
[19] Dittrich T.R. *et al* 1999 *Phys. Plasmas* **6** 2164
[20] Callahan D.A. *et al* 2008 *J. Phys.: Conf. Ser.* **112** 022021
[21] Nikroo A. *et al* 2006 *Phys. Plasmas* **13** 056302
[22] Chen K.C., Cook R.C., Huang H., Letts S.A. and Nikroo A. 2006 *Fusion Sci. Technol.* **49** 750
[23] Biener J. *et al* 2006 *Fusion Sci. Technol.* **49** 737
[24] Glenzer S.H. *et al* 2010 *Science* **327** 1228
[25] Meezan N.B. *et al* 2010 *Phys. Plasmas* **18** 056304
[26] Michel P. *et al* 2009 *Phys. Rev. Lett.* **102** 025004
[27] Michel P. *et al* 2009 *Phys Plasmas* **16** 042702
[28] Oertel J.A. *et al* 2006 *Rev. Sci. Instrum.* **77** 10E308
[29] Froula D.H. *et al* 2004 *Rev. Sci. Instrum.* **75** 4168
[30] Mackinnon A.J. *et al* 2004 *Rev. Sci. Instrum.* **75** 4183
[31] McDonald J.W., Kauffman R.L., Celeste J.R., Rhodes M.A., Lee F.D., Suter L.J., Lee A.P., Foster J.M. and Slark G. 2004 *Rev. Sci. Instrum.* **75** 3753
[32] Dewald E.L. *et al* 2004 *Rev. Sci. Instrum.* **75** 3759
[33] Glenzer S.H. *et al* 2011 *Phys. Rev. Lett.* **106** 085004
[34] Michel P. *et al* 2011 A three wavelength scheme to optimize hohlraum coupling on the National Ignition Facility *Phys. Rev.* E submitted
[35] Landen O.L. *et al* 2011 'Capsule implosion optimization during the Indirect-Drive National Ignition Campaign' *Phys. Plasmas* at press
[36] Edwards M.J. *et al* 2011 The experimental plan for cryogenic layered target implosions on the National Ignition Facility—the inertial confinement approach to fusion *Phys. Plasmas* at press
[37] Ali Z.A. *et al* 2008 *Rev. Sci. Instrum.* **79** 10E527
[38] Glebov V.Y. *et al* 2006 *Rev. Sci. Instrum.* **77** 10E715
[39] Glebov V.Y., Stoeckl C., Sangster T.C., Roberts S., Lerche R.A. and Schmid G.J. 2005 *IEEE Trans. Plasma Sci.* **33** 70–6
[40] Glebov V.Y., Stoeckl C., Sangster T.C., Roberts S., Schmid G.J., Lerche R.A. and Moran M.J. 2004 *Rev. Sci. Instrum.* **75** 3559
[41] Schmid G.J. *et al* 2003 *Rev. Sci. Instrum.* **74** 1828–31
[42] Frenje J.A. *et al* 2010 *Probing High Areal-Density Cryogenic Deuterium–Tritium Implosions Using Downscattered Neutron Spectra Measured by the Magnetic Recoil Spectrometer* (New York: AIP) No 5, p 056311
[43] Herrmann H.W. *et al* 2010 *J. Phys.: Conf. Ser.* **244** 032047
[44] Izumi N. *et al* 2010 *Rev Sci. Instrum.* **81** 10E515
[45] Hagman C., Izumi N., Bell P., Bradley D., Conder A., Eckart M., Khater H., Koch J., Moody J. and Stone G. 2010 *Rev Sci. Instrum.* **81** 10E514
[46] Koch J.A., Haan S.W. and Mancini R.C. 2004 *J. Quant. Spectrosc.* **88** 433
[47] Loomis E., Grim G., Wilde C., Wilson D.C., Wilke M., Finch J., Morgan G., Tregillis I. and Clark D. 2010 *J. Phys.: Conf. Ser.* **244** 032051
[48] Biener J. *et al* 2009 *Nucl. Fusion* **49** 112001